Primordial water and dust of the Solar System: Insights from in situ oxygen measurements of CI chondrites

Maxime Piralla, Yves Marrocchi, Maximilien Verdier-Paoletti, Lionel Vacher, Johan Villeneuve, Laurette Piani, David V Bekaert, Matthieu Gounelle

Primordial water and dust of the Solar System: Insights from *in-situ* oxygen measurements of CI chondrites

Maxime Piralla[1,*], Yves Marrocchi[1], Maximilien J. Verdier-Paoletti[2,3], Lionel G. Vacher[1,4], Johan Villeneuve[1], Laurette Piani[1], David V. Bekaert[1] and Matthieu Gounelle[2.]

[1]CRPG, CNRS, Université de Lorraine, UMR 7358, Vandoeuvre-lès-Nancy, 54501, France

[2]IMPMC, CNRS & Muséum national d'Histoire naturelle, UMR 7590, CP52, 57 rue Cuvier, 75005 Paris, France

[3]DTM, Carnegie Institution for Science, Washington, DC, 20015, USA

[4]Department of Physics, Washington University, St. Louis, MO, 63130, USA

[*]Corresponding author: Maxime Piralla (maxime.piralla5@etu.univ-lorraine.fr)

Abstract

As the chemical compositions of CI chondrites closely resemble that of the Sun's photosphere, their oxygen isotopic compositions represent a powerful tool to constrain the origin and dynamics of dust and water ice grains in the protoplanetary disk. However, parent-body alteration processes make straightforward estimation of the primordial isotopic compositions of CI chondritic water and anhydrous minerals difficult. In this contribution, we used *in-situ* SIMS measurements to determine the oxygen isotope compositions of mechanically isolated olivine and carbonate grains from the CI chondrite Orgueil and carbonates in a polished section of the CI chondrite Ivuna. Most CI olivine grains have Earth-like O isotopic compositions ($\Delta^{17}O \approx 0‰$) plotting at the intersection of the terrestrial fractionation line and the primitive chondrule minerals line. Ca-carbonates from Orgueil and Ivuna define a trend with $\delta^{17}O = (0.50 \pm 0.05) \times \delta^{18}O + (0.9 \pm 1.4)$ that differs from mass-independent variations observed in secondary phases of other carbonaceous chondrites. These data show that CIs are

chemically solar but isotopically terrestrial for oxygen isotopes. This supports models suggesting that primordial Solar System dust was ^{16}O-poor ($\Delta^{17}O \approx 0‰$) relative to the ^{16}O-rich nebular gas. Based on results, mass balance calculations reveal that the pristine O isotopic compositions of carbonaceous chondrite matrices differ significantly from the CI composition, except for CR chondrites (calculated $\Delta^{17}O$ values of CM, CO, CV and CR matrices being –3.97 ± 1.19‰, –4.33 ± 1.45‰, –7.95 ± 1.95‰, and –0.07 ± 1.16‰, respectively). This confirms an open chondrule-matrix system with respect to oxygen isotopes where chondrule compositions reflect complex processes of chondrule precursor recycling and gas-melt interactions. As the Mg-Si-Fe chondrule budget is also partially controlled by gas-melt interactions, the complementary formation of chondrules and matrix from a single solar-like reservoir −if it exists− require that (i) this reservoir must have been in a closed system with the gas or (ii) the gas had a CI composition to satisfy the elemental mass balance.

Keywords: CI chondrites, water, primordial dust, oxygen isotopes, chondrule-matrix complementarity

1. Introduction

CI carbonaceous chondrites contain the highest abundances of hydrogen (~1.5 wt.%; Alexander et al., 2012) of all chondrite classes and groups, mostly in their hydrated minerals. These minerals are considered to result from intense episodes of hydrothermal alteration induced by the melting of accreted water ice grains, which strongly modified the initial CI petrography (Brearley, 2006). CI chondrites indeed contain high abundances of secondary minerals such as phyllosilicates (81–84 vol.%), magnetites (6–10 vol.%), sulfides (4–7 vol.%), and carbonates (<3 vol.%; King et al., 2015). Although CI chondrites are the most altered chondrites known so far, they are of primary importance as their bulk chemical compositions are similar to that of the solar photosphere, which is representative of the average Solar System composition (Lodders, 2003).

Chondrites generally comprise four main components in variable proportions: chondrules (20–80 vol.%), refractory inclusions (0.1–3 vol.%), Fe-Ni metal beads (0.1–70 vol.%), and matrix material (1–75 vol.%). These different components formed during the evolution of the solar protoplanetary disk and thus represent temporal and spatial records of the formation of the Solar System. The chondrule-matrix complementarity model proposes that chondrules and matrices in carbonaceous chondrites are genetically linked based on their Mg/Si ratios (Hezel and Palme, 2010; Palme et al., 2015; Hezel et al., 2018): although bulk carbonaceous chondrites exhibit CI chondritic Mg/Si ratios, chondrules and matrices have super- and sub-CI chondritic ratios, respectively, suggesting that chondrules and matrices formed from a unique chemical reservoir of bulk CI composition. Although this model is widely debated (see Hezel et al., 2018, and Zanda et al., 2018, for recent reviews), it has fundamental implications for the dynamics of the protoplanetary disk and highlights the importance of deciphering the nature of the primitive CI matrix in terms of understanding

(i) the conditions of chondrule formation (Hezel et al., 2018; van Kooten et al., 2019) and (ii) the transport of dust in the protoplanetary disk (Anders, 1964; Zanda et al., 2018). Unfortunately, CI chondrites are rare and only a few have been described: Alais (~6 kg), Ivuna (705 g), Orgueil (~14 kg), Revelstocke (1 g), and Tonk (7.7 g). In addition, the intense parent-body fluid circulation processes that altered CI chondrites limit our knowledge of their original characteristics. Thus, it remains unclear if CI chondrites were entirely composed of fine-grained matrix or if they initially contained significant proportions of refractory inclusions, chondrules, and Fe-Ni metal beads that were subsequently erased by secondary alteration processes. To our knowledge, only one partially altered, ^{26}Al-free, ^{16}O-rich Ca-Al-rich refractory inclusion has been described in Ivuna (Frank et al., 2011, 2017), and no chondrules or pseudomorphosed chondrules have yet been reported in CI chondrites.

Although extensively altered, high-temperature minerals such as olivine and pyroxene are present in significant proportions in CI chondrites (~3 vol.%; King et al., 2015) and can be isolated by mechanical processing (Reid et al., 1970; Kerridge and MacDougall, 1976; Leshin et al., 1997) and identified in thin sections. These grains are generally anhedral and have been reported to contain Fe-Ni metal blebs and glass inclusions with shrinking bubbles (Reid et al., 1970; Kerridge and MacDougall, 1976; Leshin et al., 1997; Le Gac et al., 2009). Most olivines extracted from CI chondrites and measured by secondary ion mass spectrometry (SIMS; Leshin et al., 1997) have O isotopic compositions plotting at the intersection of the Primitive Chondrule Minerals line (PCM, $\delta^{17}O = 0.987 \times \delta^{18}O - 2.7$; Ushikubo et al., 2012) and the Terrestrial Fractionation Line (TFL, $\delta^{17}O = 0.52 \times \delta^{18}O$). Few olivine grains exhibit more ^{16}O-rich compositions (Leshin et al., 1997) similar to chondrule olivines commonly measured in CM, CO and CV carbonaceous chondrite (i.e., $\delta^{18}O \approx \delta^{17}O \approx -7‰$; Clayton and Mayeda, 1999; Marrocchi and Chaussidon, 2015; Marrocchi, et al., 2018a, 2019; Tenner et al., 2018), suggesting that chondrules might represent a significant component accreted by CI

chondrites. However, the large uncertainties on these measurements (i.e., ~4.5‰, 2σ, inherent in SIMS measurements at that time) preclude definite interpretation regarding the signature of high-temperature minerals in CI chondrites. In addition, it is not clear if CI chondrite-accretion region(s) experienced chondrule formation processes or if chondrules were radially transported from other chondrule-forming regions.

Among the secondary phases in CI chondrites, carbonates are of primary importance as they represent a direct snapshot of the alteration fluid from which they precipitated (Clayton and Mayeda, 1984). However, only a few measurements have been reported so far for carbonates in CI chondrites, and only the $\delta^{18}O$ values were reported (Grady et al., 1988; Alexander et al., 2015). In addition, these data correspond to analyses after H_3PO_4 acid treatment (Clayton and Mayeda, 1984; Leshin et al., 2001), and potential contamination from adjacent matrix cannot be excluded. To date, no SIMS O isotopic analyses have been reported for CI carbonates, despite the aptitude of this technique for deciphering the origin of water accreted by chondrites and their alteration conditions (Tyra et al., 2012, 2016; Lee et al., 2013; Fujiya et al., 2015; Vacher et al., 2016, 2017, 2019; Verdier-Paoletti et al., 2017, 2019; Jilly-Rehak et al., 2017; Marrocchi et al., 2018b).

Here, we report results from a protocol in which we have (i) mechanically isolated mafic minerals and carbonate grains from the CI chondrite Orgueil, and (ii) determined their oxygen isotopic composition by SIMS. For comparison, we surveyed a polished section of Ivuna and analysed the O isotopic compositions of carbonates. We use our results to investigate the pre-alteration oxygen isotopic composition of CI chondrites and to constrain the source of water accreted by CI chondrites. In addition, we perform mass-balance calculations to (i) estimate the pristine oxygen isotopic compositions of carbonaceous chondrite matrices and (ii) bring constraints on the controversial concept of chondrule-matrix complementary.

2. Material and methods

2.1 Grain separation and preparation

Mineral grains were separated from ~15 mg of Orgueil following the method described in Leshin et al. (1997), and briefly summarized here. Chips of Orgueil were gently crushed in an agate mortar and the powder was ultrasonically cleaned in ethanol for 45 min. After drying, the powder was sieved into <50 μm, 50–100 μm, and >100 μm size fractions. Coarse olivine and carbonate grains were then handpicked, mounted in epoxy, and polished using diamond paste (Fig. 1).

2.2 Petrographic and mineralogical characterisation

We acquired elemental distribution maps of Ivuna at the Natural History Museum in London using a Zeiss EVO 15LS scanning electron microscope (SEM) equipped with an Oxford Instruments XMax silicon drift energy dispersive X-ray (EDX) detector and INCA version 18 software (Fig. 2). Backscattered electron images and EDX maps were acquired at an accelerating voltage of 20 kV and 3 nA beam current. Due to the size of the samples (each approximately 3.5 cm^2), coverage at high resolution required the overnight collection of over 200 separate maps per section using the Smartmap automated-stage raster procedure. For each X-ray map area, multiple frames of 1024 × 768 analysis points were collected at a pixel-spacing of 1.52 μm. X-ray emission spectra (0–10 keV in 2048 channels) were stored for each pixel location. Elemental X-ray maps were subsequently extracted from the data set (approximately 1.2 GB), and combined in a conventional Mg = red, Fe = blue, Ca = green colour scheme to reveal areas of specific interest (Fig. 2).

Minerals isolated from Orgueil were coated with a 25-nm-thick carbon layer to avoid charging effects under the electron beam. SEM imaging was performed on a JEOL JSM-6510 SEM equipped with a Genesis EDX detector at the Centre de Recherches Pétrographiques et Géochimiques (CRPG-CNRS, Nancy, France) using 3 nA electron beam accelerated at 15 kV.

Quantitative chemical compositions of carbonate and olivine grains were obtained using a Cameca SX Five electron microprobe at the Université Pierre et Marie Curie (UPMC, Camparis, Paris, France) using a 40 nA focused beam accelerated to 15 kV. We analysed Na, Mg, Si, Al, K, Ca, Fe, Ti, Cr, and Mn in Orgueil olivines, Mg, Si, Ca, Fe, and Mn in Orgueil carbonates, and Na, Mg, Si, Al, K, Ca, Fe, Cr, and Mn in Ivuna carbonates. The high beam current allowed detection limits for silicates to be 150 ppm for Al, Ca, and Ti, 200 ppm for Mn and Si, and 400 ppm for Na, K, Cr, Fe, and Mg. The PAP software was used for matrix corrections. We estimate the detection limits for carbonates to be 900 ppm for Ca, Fe, Mn, Na, and K, and 600 ppm for Mg, Al, Si, and Cr.

2.3 Oxygen-isotope analysis

We measured the oxygen isotopic compositions of CI minerals via SIMS using the CAMECA IMS 1270 E7 at CRPG-CNRS. $^{16}O^-$, $^{17}O^-$, and $^{18}O^-$ ions produced by a Cs^+ primary ion beam (~15 µm, ~4 nA) were measured in multi-collection mode using three Faraday cups. A normal-incidence electron gun was used for charge compensation.

To remove interference from $^{16}OH^-$ on the $^{17}O^-$ peak and achieve maximum flatness atop the $^{16}O^-$ and $^{18}O^-$ peaks, the entrance and exit slits of the central Faraday cup were adjusted to reach a mass resolving power (MRP = M/ΔM) of ~7000 for $^{17}O^-$. $^{16}O^-$ and $^{18}O^-$ were measured on L'2 and H1 (slit 1, MRP ≈ 2500). As an additional safeguard against $^{16}OH^-$ interference, a N_2 trap was used to reduce the pressure in the analysis chamber to $<5 \times 10^{-9}$

mbar. The total measurement duration was 240 s (180 s of measurement + 60 s of pre-sputtering). We used five terrestrial standard materials (San Carlos olivine, magnetite, diopside, calcite, and dolomite) to define the instrumental mass fractionation (IMF) line for the three oxygen isotopes and correct for IMF due to matrix effects in olivine and carbonate grains. Typical count rates obtained on standards were 2.8×10^9 cps for ^{16}O, 1.1×10^6 cps for ^{17}O, and 6.3×10^6 cps for ^{18}O in carbonates, and 2.7×10^9 cps for ^{16}O, 1.0×10^6 cps for ^{17}O, and 5.5×10^6 cps for ^{18}O in San Carlos olivine. Typical 2σ measurement errors, accounting for internal errors on each measurement and the external reproducibility of the standard, were estimated to be ~0.2‰ for $\delta^{18}O$, ~0.3‰ for $\delta^{17}O$, and ~0.9‰ for $\Delta^{17}O$ (representing deviation from the TFL: $\Delta^{17}O = \delta^{17}O - 0.52 \times \delta^{18}O$).

3. Results

We found 5 olivine, 6 calcite, 14 dolomite, and 8 ferromagnesite grains in Orgueil after crushing, sieving, and handpicking (representative olivine grains are shown in Fig. 1). Additionally, we selected 16 dolomite grains in the thick section of Ivuna for chemical and isotopic characterization. Hereafter, grains are referred to using the identifiers "O" for Orgueil and "I" for Ivuna.

Orgueil olivines were Mg-rich ($Fo_{88–95}$) and had low abundances of minor elements such as Ca (≤0.2 wt.% CaO, Table 1). Four of the five olivine grains had similar O isotopic compositions plotting at the intersection of the TFL and PCM, with average values of $\delta^{18}O$ = 5.69 ± 0.42‰ and $\delta^{17}O$ = 2.96 ± 0.23‰ (Fig. 3A, Table 2). Only olivine grain O16-8 had markedly different O isotopic values ($\delta^{18}O$ = 1.14 ± 0.18‰ and $\delta^{17}O$ = –1.41 ± 0.38‰, Fig. 3A, Table 3) and plotted on the PCM below the TFL; this olivine had the highest Fo content and was enriched in Al, Ca, and Cr compared to the other olivine grains (Table 1).

We observed Ca-rich, Ca-Mg-rich, and Mg-Fe-Mn-rich carbonate groups in Orgueil, which represent calcites, dolomites, and ferromagnesites, respectively (Table 3). Based on microprobe analyses, we identified 6 calcites, 14 dolomites, and 8 ferromagnesites. The ferromagnesites include two breunnerites ($[Mg_xFe_{(1-x)}]CO_3$ with $0.7 < x < 0.9$; grains O6-2 and O7-13), five mesitites ($[Mg_xFe_{(1-x)}]CO_3$ with $0.5 < x < 0.7$; grains O6-7, O6-10, O7-8, O7-18, and O17-6), and one magnesite ($MgCO_3$, grain O21-6). Calcites in Orgueil had constant O isotopic compositions averaging $\delta^{18}O = 25.55 \pm 0.08$‰ and $\delta^{17}O = 13.29 \pm 0.36$‰ (Fig. 3A, Table 3). Dolomite grains had varying O isotopic compositions, with $\delta^{18}O$ values ranging from 24.16 to 32.49‰ and $\delta^{17}O$ values from 12.81 to 17.22‰, but constant $\Delta^{17}O$ values averaging 0.02 ± 0.80‰ (Fig. 3A, Table 3). In Ivuna, we observed only dolomites (Fig. 2) of similar isotopic compositions to Orgueil dolomites, with $\delta^{18}O$ values ranging from 24.57 to 29.66‰, $\delta^{17}O$ values from 13.06 to 15.68‰, and constant $\Delta^{17}O$ values averaging 0.40 ± 0.80‰ (Fig. 3A, Table 3).

4. Discussion

4.1 Nature and origin of CI olivine grains

All but one olivine grain isolated from Orgueil have O isotopic compositions plotting at the intersection of the PCM and TFL ($\Delta^{17}O = 0$‰, Fig. 3), which corresponds to the typical oxygen isotopic composition of olivine grains from the Earth's mantle (Eiler, 2001). In addition, these olivine grains have lower Fo contents (Fo_{88-95}) than those commonly reported in (i) CI chondrites (i.e., Fo > 95; Fig. 4; Reid et al., 1970; Kerridge and MacDougall, 1976; Steele, 1990; Leshin et al., 1997; Le Gac et al., 2009; Frank et al., 2014) and (ii) type I chondrules in different types of carbonaceous chondrites (i.e., Fo > 94; Frank, et al., 2014;

Tenner et al., 2018). This raises the question of whether these oxygen isotopic compositions reflect terrestrial contamination. However, the olivine grains were recovered after crushing a solid piece of Orgueil, and not from a powder that could have had been contaminated by terrestrial minerals. In addition, CI olivines grains with Fo < 95 are not uncommon as olivine grains with Fo as high as 55 have been reported in previous studies (Fig. 4; Reid et al., 1970; Kerridge and MacDougall, 1976; Steele, 1990; Leshin et al., 1997; Le Gac et al., 2009; Frank et al., 2014). Furthermore, among the recovered olivine grains, one plots on the PCM but below the TFL (Fig. 2), suggesting an extraterrestrial origin. Finally, previous studies of mechanically isolated mafic minerals from Orgueil reported similar olivine and pyroxene O isotopic compositions (Leshin et al., 1997). These observations suggest that the mafic minerals isolated from Orgueil indeed correspond to primary extraterrestrial minerals, in good agreement with their relative abundances in Orgueil as inferred from X-ray diffraction patterns (~3%; King et al., 2015).

CI chondrites are the only subgroup of chondrites that do not contain chondrules, not even pseudomorphosed chondrules as observed in heavily altered CM1 chondrites (Zolensky et al., 1997; Vacher et al., 2018). It has been proposed that mafic minerals mechanically isolated from CIs could correspond to chondrule fragments (McSween, 1977; Richardson and McSween, 1978; Jones, 1992; Leshin et al., 1997) or grains formed by condensation processes (Steele, 1986; Weinbruch et al., 1993). A magmatic origin for the CI olivine grains is supported by the presence of glass inclusions (Fig. 1) and normal igneous zonings within isolated olivine grains (Leshin et al., 1997). In addition, the covariation of CaO with olivine Fo content is similar to that observed within chondrules (Leshin et al., 1997; Villeneuve et al., 2015; Marrocchi et al., 2019), suggesting that chondrules could represent a potential constituent of CI chondrites. However, the presence of chondrule-like olivine grains in CI chondrites does not imply that the mechanism(s) at the origin of chondrules operated in the

CI-forming region as they could also have been inherited from other chondrule-forming regions. Interestingly, CI olivine grains show ^{17,18}O-rich isotopic compositions compared to other chondrites (Tenner et al., 2018; Marrocchi et al., 2019), at the exception of CR, ordinary and enstatite chondrites that commonly show type I chondrules with $\Delta^{17}O \approx 0$ ‰ (Schrader et al., 2013; Tenner et al., 2015, 2018). However, $\mu^{26}Mg^{*}$–$\mu^{54}Cr$ systematics of CI and CR chondrites suggest they accreted in spatially isolated regions during the evolution of the protoplanetary disk (van Kooten et al., 2016). Furthermore, chondrule olivines are extremely rare in enstatite chondrite chondrules (Piani et al., 2016) and commonly show $\Delta^{17}O > 0$ ‰ in ordinary chondrites (Tenner et al., 2018), making their contribution to the CI budget unlikely.

CI olivine grains also show similarities with crystalline silicates from comet 81P/Wild 2 samples and interplanetary dust particles (IDPs) that show a large range of Fo contents ($Fo_{60–99}$; Zolensky and Barrett, 1994; Zolensky et al., 2006; Nakamura et al., 2008; Starkey and Franchi, 2013; Frank et al., 2014). In addition, the large majority of olivine grains recovered from comet 81P/Wild 2 aerogel tracks have ^{16}O-poor isotopic compositions with $\Delta^{17}O \approx 0$‰ (Fig. 5; McKeegan et al., 2006; Nakamura et al., 2008; Ogliore et al., 2012; Defouilloy et al., 2017), similar to the $\Delta^{17}O$ values of olivine grains isolated from Orgueil and Ivuna (Leshin et al., 1997; this study). Although showing a large range of O isotopic compositions (i.e., $-40‰ < \delta^{18}O < +200‰$), IDP silicate minerals commonly cluster around the intersection of the PCM and TFL (Aléon et al., 2009; Nakashima et al., 2012; Starkey and Franchi, 2013; Starkey et al., 2014). Thus, the picture that emerges from petrographic and isotopic characterization of mafic minerals isolated from CI chondrites is that (i) chondrules could have represent a potential constituent of CIs before the onset of aqueous alteration and (ii) cometary materials could have sampled mafic minerals similar to those observed in CI chondrites.

4.2 Insights into the compositions of primordial dust and water of the Solar System

Our data represent the first reported SIMS measurements of carbonates in CI chondrites. Carbonates in both Orgueil and Ivuna plot on the TFL with mean $\Delta^{17}O$ values of 0.01 ± 0.18‰ and 0.39 ± 0.17‰, respectively (Fig. 3, Table 3). These results are similar, within errors, to those reported based on H_3PO_4 acid treatments of the whole rocks (Clayton and Mayeda, 1984; Leshin et al., 2001). Similar to the olivine grains (see section 4.1), it is unlikely that calcite and dolomite grains correspond to terrestrial contamination as Mn-Cr studies revealed systematic ^{53}Cr excesses induced by the radioactive decay of ^{53}Mn (Petitat et al., 2009, 2011; Fujiya et al., 2013). Our results thus suggest that all CI carbonates precipitated from a fluid with Earth-like O isotopic compositions (i.e., $\Delta^{17}O \approx 0$‰; Fig. 3B). In addition, CI chondrite matrices, which are largely dominated by phyllosilicates (i.e., 80–85%; King et al., 2015), show $\Delta^{17}O = 0.34$‰ (Clayton and Mayeda, 1999) that is similar within error to our results from CI Ca-carbonates (Table 2). This supports the formation of CI chondrite secondary phases from a fluid with Earth-like O isotope composition (i.e., $\Delta^{17}O \approx 0$ ‰), as also inferred from pyrolysis (Baker et al., 2002). CI chondrites thus does not show significant $^{17,18}O$ enrichments that would have been expected if the CI parent body had formed in a region of the Solar System or the parent molecular cloud where self-shielding of UV light by ^{16}O-rich nebular CO would have produced ^{16}O-poor water (Thiemens and Heidenreich, 1983; Clayton, 2002; Yurimoto and Kuramoto, 2004; Desch et al., 2018). Instead, CI water is characterized by Earth-like O isotopic compositions (Fig. 3). However, this may not represent the primordial isotopic composition of water ice grains in the CI-accreting region and does not necessarily exclude the self-shielding process. As CIs formed relatively late in the disk history (i.e., ~ 3 My after CAIs, Sugiura and Fujiya, 2014), water ice could have experienced thermal processing and O-isotope exchange with amorphous silicates

295 and CO in the protoplanetary disk. For instance, recent experimental approach points out that
296 amorphous silicate grains (i.e., the main constituent of primordial chondritic matrices; Le
297 Guillou et al., 2015) would experience oxygen isotopic exchange with water vapor within the
298 lifetime of the disk at temperatures above ~ 500-650 K (Yamamoto et al., 2019).
299 Alternatively, potentially ^{17,18}O-rich CI water could also have experienced isotopic exchange
300 on the CI, ^{16}O-rich, parent body. This would shift the water O isotope composition toward
301 Earth-like compositions as commonly observed for other chondrites (CR, CM, CV, CO; e.g.
302 Horstmann et al., 2014; Fujiya et al., 2015; Vacher et al., 2017, 2018, 2019; Verdier-Paoletti
303 et al., 2017, 2019; Jilly-Rehak et al., 2017; Marrocchi et al., 2018b). This is supported by the
304 heavy O isotope compositions of CI magnetite grains (i.e., $\Delta^{17}O$ = 1.67‰, Fig. 3B; Clayton
305 and Mayeda, 1999) that are statistically different from those of other secondary phases. Such
306 values cannot result from temperature-driven mass-dependent fractionations and thus suggest
307 that initial CI water could have had a $\Delta^{17}O$ value slightly above 0‰. However, the isotopic
308 exchange during the evolution of the CI parent body should have been limited due to the
309 small $\Delta^{17}O$ variations observed between CI magnetite and phyllosilicates + olivines (whose
310 $\Delta^{17}O$ is assumed to represent the O isotope composition of the CI anhydrous protolith). Taken
311 together, this suggests that CI parent body accreted water ice grains with Earth-like
312 composition (i.e., $\Delta^{17}O \approx 0$).

313 CI anhydrous silicates also show terrestrial values ($\Delta^{17}O \approx 0$‰; Fig. 3), implying that
314 the different constituents of CI chondrites all had Earth-like O isotopic compositions.
315 Although CI chondrites are slightly depleted in oxygen relative to the Sun's photosphere
316 (Lodders, 2003), our data show that CIs are chemically solar but isotopically terrestrial for
317 oxygen isotopes. Interestingly, this is not the case for non-traditional isotopic system (e.g.,
318 ^{50}Ti, ^{54}Cr; Dauphas 2017). However, our results provide a strong argument in favor of a
319 scenario where the primordial dust of the Solar System would have been ^{16}O-poor (with $\Delta^{17}O$

≈ 0) relative to the ^{16}O-rich nebular gas (Krot et al., 2010). In this scenario, ^{16}O-rich and ^{16}O-poor reservoirs could have co-existed in the protoplanetary disk, with nebular regions characterized by enhanced dust/gas ratios being ^{16}O-poor relative to solar due to the overabundance of ^{16}O-poor solids. Our data thus suggest that primordial Solar System dust could correspond to CI-like material characterized by a ^{16}O-poor isotopic composition.

4.3 δ^{17}O-δ^{18}O of primordial CI matrix - Implications on chondrule-matrix complementary

Understanding the potential genetic link between chondrules and chondritic matrices is fundamental, as it would bring invaluable constraints on the origin of dust in the protoplanetary disk. Based on their elemental compositions (Hezel and Palme, 2010; Palme et al., 2015; Hezel et al., 2017, 2018), it has been proposed that the chondrules and matrices of carbonaceous chondrites formed simultaneously from the same solar-like reservoir. These reservoirs would have had major element compositions (i.e., Mg, Si, and Fe) similar to CI chondrites, but with variable degrees of depletion in volatile elements depending on the chondrite group (Hezel and Palme, 2010; Palme et al., 2015; Hezel et al., 2018). Chondrule-matrix complementarity has recently been supported by tungsten isotopic measurements of the matrix and chondrules in Allende (Budde et al., 2016). However, the intrinsic nature, and indeed the existence, of the chondrule-matrix complementarity are hotly debated. Alternative models propose that bulk chondrite compositions are better reproduced by considering (i) a non-CI complementarity (Bland et al., 2005) or (ii) a unique CI-composition matrix added to various amounts of chondrules (Anders, 1964; Zanda et al., 2018). The latter model implies that chondrules and chondritic matrices are not genetically related, but formed in different reservoirs (Zanda et al., 2018).

This complementarity is not straightforward for oxygen isotopes as the chondrule oxygen isotopic compositions show large intra- and inter-chondrule variations (Clayton and Mayeda, 1984; Marrocchi and Chaussidon, 2015; Tenner et al., 2018) requiring at least three reservoirs (Palme et al., 2015). However, the matrices accreted by the different groups of carbonaceous chondrites experienced secondary alteration processes under varying conditions (Brearley, 2006; Le Guillou et al., 2015; Vacher et al., 2017; Ganino and Libourel, 2017; Marrocchi et al., 2018b) that affected their O isotopic signatures and now preclude straightforward determination of their initial compositions. Thus, based on our data, we calculated the isotopic compositions of the different carbonaceous chondrite (hereafter, CC) matrices before the onset of alteration by considering the following. It has been shown that CM, CO, CR, and CV bulk O isotopic compositions have well-defined trends in a $\delta^{17}O$-$\delta^{18}O$ diagram that correspond to variable extents of isotopic exchange between a ^{16}O-rich anhydrous protolith and $^{17,18}O$-rich water (Clayton and Mayeda, 1984; Marrocchi et al., 2018b; Fujiya, 2018). We calculated the coordinates of the intersections of these respective trends with the PCM, which correspond to the bulk anhydrous O isotopic compositions of the different CCs before overprinting by parent-body processes (see Fig. 6 for a schematic example, Table 4). Importantly, none of the CC groups investigated here has the same bulk anhydrous O isotopic composition as CIs (Fig. 7A, Table 4). By considering the modal abundances of Ca-Al-rich inclusions (CAIs), chondrules, and matrix in the different CCs (Scott and Krot, 2014), we calculated the $\Delta^{17}O$ values of the respective pre-alteration matrices accreted by the different CCs, assuming that (i) CAIs have an average $\Delta^{17}O$ value of –25‰ (Kawasaki et al., 2017; Aléon, 2018), (ii) chondrules have variable $\Delta^{17}O$ values in the range of –6 to –2‰ (Tenner et al., 2018), and (iii) CAIs, chondrules, and matrices have similar oxygen contents.

This calculation reveals that the pristine O isotopic compositions of CC matrices differed significantly from that of CIs ($\Delta^{17}O$ values of CM, CO, and CV matrices being –3.97 ± 1.19‰, –4.33 ± 1.45‰, and –7.95 ± 1.95‰, respectively), except for CR matrices, which had a $\Delta^{17}O$ value of –0.07 ± 1.16‰ (Fig. 7B, Table 4). This result confirms that the complementarity concept cannot be applied to oxygen, mainly because chondrules were formed through complex processes of precursor recycling and gas-melt interactions (Tissandier et al., 2002; Hezel et al., 2006; Libourel et al., 2006; Schrader et al., 2013, 2018; Marrocchi and Libourel, 2013; Marrocchi and Chaussidon, 2015; Friend et al., 2016; Marrocchi et al., 2016; Piani et al., 2016). Hence, in the framework of the complementarity model, the oxygen budget of carbonaceous chondrites can be written as:

$$O_{Bulk\ CC} = O_{Chondrules} + O_{Matrix} \quad (1)$$

with

$$O_{Chondrules} = O_{Precursors} + O_{Gas} \quad (2)$$

and

$$\Delta^{17}O_{Matrix}\ (CC) \neq \Delta^{17}O_{Matrix}\ (CI) \quad (3)$$

However, recent studies have demonstrated that partially molten chondrule precursors experienced protracted gas-melt interactions with gaseous SiO and Mg (Libourel and Portail, 2018; Marrocchi et al., 2018a; Marrocchi et al., 2019). In addition, mass balance calculations based on the abundance of sulfides in CV chondrules suggest that about half of their total Fe content originated from the gas phase (Marrocchi and Libourel, 2013). These constraints suggest that the Mg-Si-Fe budget was strongly affected by gas-melt interactions in the same way as oxygen:

$$(Mg, Si, Fe)_{Bulk\ CC} = (Mg, Si, Fe)_{Chondrules} + (Mg, Si, Fe)_{Matrix} \quad (4)$$

with

$$(\mathrm{Mg, Si, Fe})_{\mathrm{Chondrules}} = (\mathrm{Mg, Si, Fe})_{\mathrm{Precursors}} + (\mathrm{Mg, Si, Fe})_{\mathrm{Gas}} \quad (5)$$

If chondrules and matrices formed complementarily from the same reservoir, this implies that (i) this reservoir must have been in a closed system with the gas itself, or (ii) the gas was of CI composition to satisfy the Mg-Si-Fe elemental mass balance. In the protoplanetary disk, the canonical dust to gas ratio is commonly taken as ~10^{-2} (Birnstiel et al., 2010), meaning that the condensation of solids and their subsequent interactions with the gas should not have significantly affected the composition of the gas, which should have maintained, by definition, a solar composition. However, given that disk evolution and differential dynamical coupling with the gas motion depends on grain size, the dust/gas ratio was probably heterogeneous, with chondrules having potentially formed under a large range of dust enhancements (Cuzzi et al., 2008; Alexander et al., 2012; Marrocchi and Chaussidon, 2015). In such dusty regions, rapid heating and evaporation of the dust could have lead to environments where the gas had a predominantly CI-like composition.

It has recently been proposed that chondrules result from the recycling of previously condensed amoeboid olivine aggregates (AOAs; Jacquet and Marrocchi, 2017; Marrocchi et al., 2018a; Marrocchi et al., 2019). This implies that AOAs experienced rapid and efficient transport through regions of the protoplanetary disk where the gaseous reservoir was ^{17,18}O-enriched relative to their condensation zones (Marrocchi et al., 2019). This outward transport of AOAs could have been achieved through viscous spreading, as recently proposed for CAIs (Nanne et al., 2019). However, maintaining a closed (chondrule + gas + matrix) system at the scale of the protoplanetary disk to satisfy the (O, Mg, Si, Fe) mass balance appears unrealistic and imposes important constraints on the complementarity model. Interestingly, large-scale isotopic heterogeneities within the disk, such as the non-carbonaceous–carbonaceous

chondrite nucleosynthetic dichotomy (Kruijer et al., 2017; Gerber et al., 2017; Nanne et al., 2019), could reflect internal heterogeneities within the Solar System's parental molecular cloud itself, with different regions of the nascent disk receiving variable compositions of infalling material (Nanne et al., 2019). This supports models where the O isotopic heterogeneity of the Solar System was partially established by self-shielding in the molecular cloud (Yurimoto and Kuramoto, 2004). Such complex gas-melt interactions during chondrule formation should be better accounted for to improve our understanding of the potential chondrule-matrix complementarity.

Conclusions

We have performed *in-situ* SIMS oxygen isotopic analyses of olivines and carbonates in the CI chondrites Orgueil and Ivuna. Our main results are:

1. All olivine grains but one show O isotopic compositions plotting at the intersection of the TFL and PCM.

2. Ca-carbonates describe a trend with $\delta^{17}O = (0.50 \pm 0.05) \times \delta^{18}O + (0.9 \pm 1.4)$ that differs from mass-independent variation observed in secondary phases of other carbonaceous chondrites.

From these data, we drew the following interpretations:

1. Olivine grains isolated from Orgueil could correspond to chondrule fragments.

2. The O isotopic compositions of CI anhydrous solids and water show Earth-like values, thus defining a fundamental characteristic of CIs that appear to be chemically solar but isotopically terrestrial for oxygen isotopes.

3. The ^{16}O-poor composition of CI anhydrous dust particles supports models where primordial Solar System dust is characterized by terrestrial values ($\Delta^{17}O \approx 0‰$).

4. Anhydrous bulk O isotopic compositions of CCs are distinct from the anhydrous CI bulk composition. Likewise, the pre-alteration O isotopic composition of the CI matrix is different from those of CCs, except for CR chondrites. This highlights that matrix-chondrule complementarity does not apply to oxygen isotopes, possibly as the result of complex gas-melt interactions during chondrule formation within the protoplanetary disk.

5. Recent chondrule formation models have proposed that complex interactions between chondrule precursors and Mg-Si-Fe-rich gas are fundamental for establishing chondrule characteristics. If chondrules and matrix formed complementarily from the same reservoir, either the reservoir must have been in a closed system with the gas or the gas must have been of CI composition to satisfy Mg-Si-Fe elemental mass balance.

6. Chondrules experienced gas-melt interactions with a ^{17,18}O-rich gaseous reservoir that differs significantly from the ^{16}O-rich isotopic composition of chondrule precursors. Assuming a spatial origin of these isotopic variations, rapid and efficient transport toward ^{17,18}O-enriched regions could have been achieved through viscous spreading, as recently proposed for CAIs. However, maintaining a closed (chondrule + gas + matrix) system at the scale of the protoplanetary disk to satisfy the (O, Mg, Si, Fe) mass balance puts important constraints on the complementarity model.

Acknowledgments

Nordine Bouden, Michel Fialin, and Nicolas Rividi are thanked for their technical assistance. Martin Lee and an anonymous are thanked for constructive comments and Associate Editor Sasha Krot for careful editing. This research was funded by l'Agence Nationale de la

Recherche through grant ANR-587 14-CE33-0002-01 SAPINS (PI Yves Marrocchi). This is CRPG-CNRS contribution #2704.

Research data

Original data of this study are available at Mendeley Data (Marrocchi and Piralla, 2019); http://dx.doi.org/10.17632/9xws4jx4fz.2.

References

Aléon J. (2018) Closed system oxygen isotope redistribution in igneous CAIs upon spinel dissolution. Earth Planet. Sci. Lett. 482, 324–333.

Aléon J., Engrand C., Leshin L. A. and McKeegan K. D. (2009) Oxygen isotopic composition of chondritic interplanetary dust particles: A genetic link between carbonaceous chondrites and comets. Geochim. Cosmochim. Acta 73, 4558–4575.

Alexander C. M. O'D, Bowden R., Fogel M. L., Howard K. T., Herd C. D. K. and Nittler L. R. (2012) The Provenances of Asteroids, and Their Contributions to the Volatile Inventories of the Terrestrial Planets. Science 337, 721–723.

Alexander C. M. O'D, Bowden R., Fogel M. L. and Howard K. T. (2015) Carbonate abundances and isotopic compositions in chondrites. Meteorit Planet Sci 50, 810–833.

Anders E. (1964) Origin, age, and composition of meteorites. Space Sci Rev 3, 583–714.

Baker L., Franchi I. A., Wright I. P. and Pillinger C. T. (2002) The oxygen isotopic composition of water from Tagish Lake: Its relationship to low- temperature phases and to other carbonaceous chondrites. Meteoritics & Planetary Science 37, 977–985.

Birnstiel T., Dullemond C.P. and Brauer F. (2010) Gas- and dust evolution in protoplanetary disk. Astron. & Astrophys. 513, A79, 21 pp.

Bland P. A., Alard O., Benedix G. K., Kearsley A. T., Menzies O. N., Watt L. E. and Rogers N. W. (2005) Volatile fractionation in the early solar system and chondrule/matrix complementarity. Proceedings of the National Academy of Sciences 102, 13755–13760.

Brearley, A.J., 2006. The action of water. *Meteorites and the Early Solar System II*. (eds. Lauretta D. S. and McSween H. Y. Tucson, Arizona: The University of Arizona Press. pp. 587–624.

Budde G., Kleine T., Kruijer T. S., Burkhardt C. and Metzler K. (2016) Tungsten isotopic constraints on the age and origin of chondrules. Proceedings of the National Academy of Sciences 113, 2886–2891.

Clayton R. N. (2002) Solar System: Self-shielding in the solar nebula. Nature 415, 860–861.

Clayton R. N. and Mayeda T. K. (1984) The oxygen isotope record in Murchison and other carbonaceous chondrites. Earth Planet. Sci. Lett. 67, 151–161.

Clayton, R.N., Mayeda, T.K., 1999. Oxygen isotope studies of carbonaceous chondrites. Geochim. Cosmochim. Acta 63, 2089–2104.

Cuzzi J. N., Hogan R. C. and Shariff K. (2008) Toward planetesimals: Dense chondrule clumps in the protoplanetary nebula. The Astrophysical Journal 687, 1432–1447.

Dauphas N. (2017) The isotopic nature of the Earth's accreting material through time. *Nature 541*, 521-524.

Defouilloy C., Nakashima D., Joswiak D. J., Brownlee D. E., Tenner T. J. and Kita N. T. (2017) Origin of crystalline silicates from Comet 81P/Wild 2: Combined study on their oxygen isotopes and mineral chemistry. Earth Planet. Sci. Lett. 465, 145–154.

Desch S.J., Kalyaan A. and Alexander C. M. O'D (2018) The Effect of Jupiter's Formation on the Distribution of Refractory Elements and Inclusions in Meteorites. The Astrophysical J. 238, 31.

Eiler J. M. (2001) Oxygen Isotope Variations of Basaltic Lavas and Upper Mantle Rocks. Reviews in Mineralogy and Geochemistry 43, 319–364.

Frank D. R., Zolensky M. E. and Le L. (2014) Olivine in terminal particles of Stardust aerogel tracks and analogous grains in chondrite matrix. Geochim. Cosmochim. Acta 142, 240-259.

Frank D., Zolensky M., Martinez J., Mikouchi T., Ohsumi K., Hagiya K., Satake W., Le L., Ross D. and Peslier A. (2011) A CAI in the Ivuna CI1 chondrite. *Lunar Planet. Sci. 47*. Lunar Planet. Inst., Houston. #1608.

Friend P., Hezel D. C. and Mucerschi D. (2016) The conditions of chondrule formation, Part II: Open system. Geochim. Cosmochim. Acta 173, 198–209.
Fujiya W. (2018) Oxygen isotopic ratios of primordial water in carbonaceous chondrites. Earth Planet. Sci. Lett. 481, 264–272.
Fujiya W., Sugiura N., Sano Y. and Hiyagon H. (2013) Mn–Cr ages of dolomites in CI chondrites and the Tagish Lake ungrouped carbonaceous chondrite. Earth Planet. Sci. Lett. 362, 130–142.
Fujiya W., Sugiura N., Marrocchi Y., Takahata N., Hoppe P., Shirai K., Sano Y. and Hiyagon H. (2015) Comprehensive study of carbon and oxygen isotopic compositions, trace element abundances, and cathodoluminescence intensities of calcite in the Murchison CM chondrite. Geochim. Cosmochim. Acta 161, 101–117.
Ganino C. and Libourel G. (2017) Reduced and unstratified crust in CV chondrite parent body. Nat Comms, 1–10.
Gerber S., Burkhardt C., Budde G., Metzler K. and Kleine T. (2017) Mixing and Transport of Dust in the Early Solar Nebula as Inferred from Titanium Isotope Variations among Chondrules. The Astrophysical Journal Letters 841, 1–7.
Gounelle M. (2011) The Asteroid-Comet Continuum: In Search of Lost Primitivity. Elements 7, 29–34.
Gounelle M., Spurný P. and Bland P. A. (2006) The orbit and atmospheric trajectory of the Orgueil meteorite from historical records. Meteoritics & Planetary Science 41, 135–150.
Grady M. M., Wright I. P., Swart P. K. and Pillinger C. T. (1988) The carbon and oxygen isotopic composition of meteoritic carbonates. Geochim. Cosmochim. Acta 52, 2855–2866.
Guo W. and Eiler J. M. (2007) Temperatures of aqueous alteration and evidence for methane generation on the parent bodies of the CM chondrites. Geochim. Cosmochim. Acta 71, 5565–5575.
Hezel D. C. and Palme H. (2010) The chemical relationship between chondrules and matrix and the chondrule matrix complementarity. Earth Planet. Sci. Lett. 294, 85–93.
Hezel D. C., Harak M. and Libourel G. (2017) What we know about elemental bulk chondrule and matrix compositions: Presenting the Chondrite DB Database. Chemie der Erde - Geochemistry, 91-121.
Hezel D. C., Bland P. A., Palme H., Jacquet E. and Bigolski J. (2018) Composition of Chondrules and Matrix and Their Complementary Relationship in Chondrites. In: Chondrules. Cambridge University Press, pp 196-246, 441 pp.
Hezel D. C., Palme H., Nasdala L. and Brenker F. E. (2006) Origin of SiO_2-rich components in ordinary chondrites. Geochim. Cosmochim. Acta 70, 1548–1564.
Horstmann M., Vollmer C., Birth M. I. F., Chaussidon M., Gurenko A. and Bischoff A. (2014) Tracking aqueous alteration of CM chondrites—Insight from in-situ oxygen isotope measurements of calcite. *Lunar Planet. Sci. 45*. Lunar Planet. Inst., Houston. #1761.
Hsieh H. H. and Jewitt D.J. (2006) A population of comets in the main asteroid belt. Science 312, 561-563.
Jacquet E. and Marrocchi Y. (2017) Chondrule heritage and thermal histories from trace element and oxygen isotope analyses of chondrules and amoeboid olivine aggregates. Meteorit Planet Sci 58, 3451–23.
Jilly-Rehak C. E., Huss G. R., Nagashima K. and Schrader D. L. (2017) Low-temperature aqueous alteration on the CR chondrite parent body: implications from in situ oxygen-isotope analyses. Geochim. Cosmochim. Acta 222, 230-252.
Jones R. H. (1992) On the relationship between isolated and chondrule olivine grains in the carbonaceous chondrite ALHA 77307. Geochim. Cosmochim. Acta 56, 3593.

Kawasaki N., Itoh S., Sakamoto N. and Yurimoto H. (2017) Chronological study of oxygen isotope composition for the solar protoplanetary disk recorded in a fluffy Type A CAI from Vigarano. Geochim. Cosmochim. Acta 201, 83–102.

Kerridge J. F. and MacDougall J. D. (1976) Mafic silicates in the Orgueil carbonaceous meteorite. Earth Planet. Sci. Lett. 29, 341–348.

King A. J., Schofield P. F., Howard K. T. and Russell S. S. (2015) Modal mineralogy of CI and CI-like chondrites by X-ray diffraction. Geochim. Cosmochim. Acta 165, 148–160.

Krot A. N., Nagashima K., Ciesla F. J., Meyer B. S., Hutcheon I. D., Davis A. M., Huss G. R. and Scott E. R. D. (2010) Oxygen isotopic composition of the sun and mean oxygen isotopic composition of the protosolar silicate dust: evidence from refractory inclusions. Astrophys. J. 713, 1159–1166.

Kruijer T. S., Burkhardt C., Budde G. and Kleine T. (2017) Age of Jupiter inferred from the distinct genetics and formation times of meteorites. Proceedings of the National Academy of Sciences 114, 6712-6716.

Le Gac Y., Benedix G. K., Science P. B. A. P. (2009) Are CI Chondrites Cometary Samples? Olivine as a Diagnostic Tool. 72th Meteoritics and Planetary Science Conference, 5242.

Le Guillou C., Changela H. G. and Brearley A. J. (2015) Widespread oxidized and hydrated amorphous silicates in CR chondrites matrices: Implications for alteration conditions and H2 degassing of asteroids. Earth Planet. Sci. Lett. 420, 162–173.

Lee M. R., Sofe M. R., Lindgren P., Starkey N. A. and Franchi I. A. (2013) The oxygen isotope evolution of parent body aqueous solutions as recorded by multiple carbonate generations in the Lonewolf Nunataks 94101 CM2 carbonaceous chondrite. Geochim. Cosmochim. Acta 121, 452–466.

Le Guillou C., Changela H. G. and Brearley A. J. (2015) Widespread oxidized and hydrated amorphous silicates in CR chondrites matrices: Implications for alteration conditions and H_2 degassing of asteroids. *Earth Planet. Sci. Lett.* **420**, 162–173.

Leshin L. A., Rubin A. E. and McKeegan K. D. (1997) The oxygen isotopic composition of olivine and pyroxene from CI chondrites. Geochim. Cosmochim. Acta 61, 835–845.

Leshin L. A., Farquhar J. and Guan Y. (2001) Oxygen isotopic anatomy of Tagish Lake: Relationship to primary and secondary minerals in CI and CM chondrites. *Lunar Planet. Sci. 32*. Lunar Planet. Inst., Houston. #1843.

Levison H. F., Bottke W. F., Gounelle M., Morbidelli A., Nesvorný D. and Tsiganis K. (2009) Contamination of the asteroid belt by primordial trans-Neptunian objects. 460, 364–366.

Libourel G. and Portail M. (2018) Chondrules as direct thermochemical sensors of solar protoplanetary disk gas. Science Advances 4, eaar3321.

Libourel G., Krot A. and Tissandier L. (2006) Role of gas-melt interaction during chondrule formation. Earth and Planetary Science Letters 251, 232–240.

Lodders K. (2003) Solar system abundances and condensation temperatures of the elements. The Astrophysical Journal 591, 1220–1247.

Marrocchi Y. and Chaussidon M. (2015) A systematic for oxygen isotopic variation in meteoritic chondrules. Earth Planet. Sci. Lett. 430, 308–315.

Marrocchi Y. and Libourel G. (2013) Sulfur and sulfides in chondrules. Geochim. Cosmochim. Acta 119, 117–136.

Marrocchi Y., Villeneuve J., Batanova V., Piani L. and Jacquet E. (2018a) Oxygen isotopic diversity of chondrule precursors and the nebular origin of chondrules. Earth Planet. Sci. Lett. 496, 132–141.

Marrocchi Y., Bekaert D. V. and Piani L. (2018b) Origin and abundance of water in carbonaceous asteroids. Earth and Planetary Science Letters 482, 23–32.

Marrocchi Y., Chaussidon M., Piani L. and Libourel G. (2016) Early scattering of the solar protoplanetary disk recorded in meteoritic chondrules. Science Advances 2, e1601001–e1601001.

Marrocchi Y., Euverte R., Villeneuve J., Batanova V., Welsch B., Ferrière L. and Jacquet E. (2019) Formation of CV chondrules by recycling of amoeboid olivine aggregate-like precursors. Geochim. Cosmochim. Acta 247, 121–141.

[dataset] Marrocchi Y. & Piralla M. (2019), "CI chondrites - Piralla", Mendeley Data, V2 http://dx.doi.org/10.17632/9xws4jx4fz.2

McKeegan K. D., Aléon J., Bradley J., Brownlee D., Busemann H., Butterworth A., Chaussidon M., Fallon S., Floss C., Gilmour J., Gounelle M., Graham G., Guan Y., Heck P. R., Hoppe P., Hutcheon I. D., Huth J., Ishii H., Ito M., Jacobsen S. B., Kearsley A., Leshin L. A., Liu M. C., Lyon I., Marhas K., Marty B., Matrajt G., Meibom A., Messenger S., Mostefaoui S., Mukhopadhyay S., Nakamura-Messenger K., Nittler L., Palma R., Pepin R. O., Papanastassiou D. A., Robert F., Schlutter D., Snead C. J., Stadermann F. J., Stroud R., Tsou P., Westphal A., Young E. D., Ziegler K., Zimmermann L. and Zinner E. (2006) Isotopic Compositions of Cometary Matter Returned by Stardust. Science 314, 1724–1728.

McSween H. Y. (1977) On the nature and origin of isolated olivine grains in carbonaceous chondrites. Geochim. Cosmochim. Acta 41, 411–418.

Nakamura T., Noguchi T., Tsuchiyama A., Ushikubo T., Kita N. T., Valley J. W., Zolensky M. E., Kakazu Y., Sakamoto K., Mashio E., Uesugi K. and Nakano T. (2008) Chondrule-like Objects in Short-Period Comet 81P/Wild 2. Science 321, 1664–1667.

Nakashima D., Ushikubo T., Zolensky M. E. and Kita N. T. (2012) High precision oxygen three-isotope analyses of anhydrous chondritic interplanetary dust particles. Meteoritics & Planetary Science 47, 197–208.

Nanne J. A. M., Nimmo F., Cuzzi J. N. and Kleine T. (2019) Origin of the non-carbonaceous–carbonaceous meteorite dichotomy. Earth Planet. Sci. Lett. 511, 44–54.

Nittler L. R., Davidson J., Liu N., Alexander C. M. O. D. and Stroud R. M. (2015) A Search for Cosmic Symplectite in the Acfer 094 and Miller Range 07687 Meteorites. *Lunar Planet. Sci. 46*. Lunar Planet. Inst., Houston. #1832.

Ogliore R. C., Huss G. R., Nagashima K., Butterworth A. L., Gainsforth Z., Stodolna J., Westphal A. J., Joswiak D. and Tyliszczak T. (2012) Incorporation of a late-forming chondrule into comet wild 2. Astrophys. J. Lett. 745, L19–5.

Palme H., Hezel D. C. and Ebel D. S. (2015) The origin of chondrules: Constraints from matrix composition and matrix-chondrule complementarity. Earth Planet. Sci. Lett. 411, 11–19.

Petitat M., McKeegan K., Sci M. G. L. P.2009 Duration and sequence of carbonate crystallization on the Orgueil protolith: ^{53}Mn–^{53}Cr systematics of their evolution in O and C isotopic composition. *Lunar Planet. Sci. 40*. Lunar Planet. Inst., Houston. #1657.

Petitat M., Marrocchi Y., McKeegan K. D., Mostefaoui S., Meibom A., Zolensky M. E. and Gounelle M. (2011) 53Mn-53Cr ages of Kaidun carbonates. Meteoritics & Planetary Science 46, 275–283.

Piani L., Marrocchi Y., Libourel G. and Tissandier L. (2016) Magmatic sulfides in the porphyritic chondrules of EH enstatite chondrites. Geochim. Cosmochim. Acta 195, 84–99.

Reid A. M., Bass M. N., Fujita H., Kerridge J. F. and Fredriksson K. (1970) Olivine and pyroxene in the Orgueil meteorite. Geochim. Cosmochim. Acta 34, 1253–1255.

Richardson S. M. and McSween H. Y. (1978) Textural evidence bearing on the origin of isolated olivine crystals in C2 carbonaceous chondrites. Earth Planet. Sci. Lett. 37, 485–491.

Rowe M. W., Clayton R. N. and Mayeda T. K. (1994) Oxygen isotopes in separated components of CI and CM meteorites. Geochim. Cosmochim. Acta 58, 5341–5347.

Sakamoto N., Seto Y., Itoh S., Kuramoto K., Fujino K., Nagashima K., Krot A. N. and Yurimoto H. (2007) Remnants of the Early Solar System Water Enriched in Heavy Oxygen Isotopes. Science 317, 231–233.

Schrader D. L., Connolly H. C. Jr, Lauretta D. S., Nagashima K., Huss G. R., Davidson J. and Domanik K. J. (2013) The formation and alteration of the Renazzo-like carbonaceous chondrites II: Linking O-isotope composition and oxidation state of chondrule olivine. Geochim. Cosmochim. Acta 101, 302–327.

Schrader D. L., Nagashima K., Waitukaitis S. R., Davidson J., McCoy T. J., Connolly H. C. and Lauretta D. S. (2018) The retention of dust in protoplanetary disks: Evidence from agglomeratic olivine chondrules from the outer Solar System. Geochim. Cosmochim. Acta 223, 405–421.

Scott E. R. D. and Krot A. N. (2014) Chondrites and Their Components. In Meteorites and Cosmochemical Processes pp. 65–137.

Seto Y., Sakamoto N., Fujino K., Kaito T., Oikawa T. and Yurimoto H. (2008) Mineralogical characterization of a unique material having heavy oxygen isotope anomaly in matrix of the primitive carbonaceous chondrite Acfer 094. Geochim. Cosmochim. Acta 72, 2723–2734.

Starkey N. A. and Franchi I. A. (2013) Insight into the silicate and organic reservoirs of the comet forming region. Geochim. Cosmochim. Acta 105, 73–91.

Starkey N. A., Franchi I. A. and Lee M. R. (2014) Isotopic diversity in interplanetary dust particles and preservation of extreme ^{16}O-depletion. Geochim. Cosmochim. Acta 142, 115–131.

Steele I. M. (1986) Compositions and textures of relic forsterite in carbonaceous and unequilibrated ordinary chondrites. Geochim. Cosmochim. Acta 50, 1379–1395.

Steele I.M. 1990. Minor elements in forsterites of Orgueil (C1), Alais (C1) and two interplanetary dust particles compared to C2-C3-UOC forsterites. *Meteoritics and Planetary Science* **25**, 301-307.

Tenner T. J., Nakashima D., Ushikubo T., Kita N. T. and Weisberg M. K. (2015) Oxygen isotope ratios of FeO-poor chondrules in CR3 chondrites: Influence of dust enrichment and H_2O during chondrule formation. Geochim. Cosmochim. Acta 148, 228–250.

Tenner T. J., Ushikubo T., Nakashima D., Schrader D. L., Weisberg M. K., Kimura M. and Kita N. T. (2018) Oxygen Isotope Characteristics of Chondrules from Recent Studies by Secondary Ion Mass Spectrometry. In: Chondrules. Cambridge University Press, pp 196-246, 441 pp.

Thiemens M. H. and Heidenreich J. E. (1983) The Mass-Independent Fractionation of Oxygen: A Novel Isotope Effect and Its Possible Cosmochemical Implications. Science 219, 1073–1075.

Tissandier L., Libourel G. and Robert F. (2002) Gas-melt interactions and their bearing on chondrule formation. Meteoritics & Planetary Science 37, 1377–1389.

Tyra M. A., Farquhar J., Guan Y. and Leshin L. A. (2012) An oxygen isotope dichotomy in CM2 chondritic carbonates: A SIMS approach. Geochim. Cosmochim. Acta 77, 383–395.

Tyra M., Brearley A. and Guan Y. (2016) Episodic carbonate precipitation in the CM chondrite ALH 84049: An ion microprobe analysis of O and C isotopes. Geochim. Cosmochim. Acta 175, 195–207.

Ushikubo T., Kimura M., Kita N. T. and Valley J. W. (2012) Primordial oxygen isotope reservoirs of the solar nebula recorded in chondrules in Acfer 094 carbonaceous chondrite. Geochim. Cosmochim. Acta 90, 242–264.

Vacher L. G., Marrocchi Y., Verdier-Paoletti M. J., Villeneuve J. and Gounelle M. (2016) Inward radial mixing of interstellar water ices in the solar protoplanetary disk. The Astrophysical Journal Letters 827, 1–6.

720 Vacher L. G., Marrocchi Y., Villeneuve J., Verdier-Paoletti M. J. and Gounelle M. (2017)
721 Petrographic and C & O isotopic characteristics of the earliest stages of aqueous alteration of
722 CM chondrites. Geochim. Cosmochim. Acta 213, 271–290.
723 Vacher L. G., Marrocchi Y., Villeneuve J., Verdier-Paoletti M. J. and Gounelle M. (2018)
724 Collisional and alteration history of the CM parent body. Geochim. Cosmochim. Acta 239,
725 213–234.
726 Vacher L.G., Piralla M., Gounelle M., Bizzarro M. and Marrocchi Y., Thermal evolution of
727 hydrated asteroids inferred from oxygen isotopes. *The Astrophysical Journal Letters 882*,
728 L20.
729 van Kooten E.M.M.E., Moynier F. and Agranier A. (2019) A unifying model for the accretion
730 of chondrules and matrix. *PNAS*, pnas.1907592116.
731 Verdier-Paoletti M. J., Marrocchi Y., Avice G., Roskosz M., Gurenko A. and Gounelle M.
732 (2017) Oxygen isotope constraints on the alteration temperatures of CM chondrites. Earth
733 Planet. Sci. Lett. 458, 273–281.
734 Verdier-Paoletti M.J., Marrocchi Y., Vacher L.G., Gattacceca J., Gurenko A., Sonzogni C. &
735 Gounelle M. (2019). Testing the genetic relationship between fluid alteration and
736 brecciation in CM chondrites. Meteoritics & Planetary Science 54, 1692-1709.
737 Villeneuve J., Libourel G. and Soulié C. (2015) Relationships between type I and type II
738 chondrules: Implications on chondrule formation processes. Geochim. Cosmochim. Acta
739 160, 277–305.
740 Weinbruch S., Zinner E. K. and El Goresy A. (1993) Oxygen isotopic composition of
741 individual olivine grains from the Allende meteorite. Geochim. Cosmochim. Acta 57,
742 2649–2661.
743 Yurimoto H. and Kuramoto K. (2004) Molecular cloud origin for the oxygen isotope
744 heterogeneity in the solar system. Science 305, 1763–1766.
745 Zanda B., Lewin E. and Humayun M. (2018) The Chondritic Assemblage. In Chondrules:
746 Records of Protoplanetary Disk Processes Complementarity Is Not a Required Hypothesis.
747 In: Chondrules. Cambridge University Press pp. 122–150.
748 Zolensky M. E. and Barrett R. A. (1994) Compositional variations of olivines and pyroxenes
749 in chondritic interplanetary dust particles. Meteoritics & Planetary Science 29, 616–620.
750 Zolensky M. E., Mittlefehldt D. W. and Lipschutz M. E. (1997) CM chondrites exhibit the
751 complete petrologic range from type 2 to 1. Geochim. Cosmochim. Acta 61, 5099–5115.
752 Zolensky M. E., Zega T. J., Yano H., Wirick S., Westphal A. J., Weisberg M. K., Weber I.,
753 Warren J. L., Velbel M. A., Tsuchiyama A., Tsou P., Toppani A., Tomioka N., Tomeoka
754 K., Teslich N., Taheri M., Susini J., Stroud R., Stephan T., Stadermann F. J., Snead C. J.,
755 Simon S. B., Simionovici A., See T. H., Robert F., Rietmeijer F. J. M., Rao W., Perronnet
756 M. C., Papanastassiou D. A., Okudaira K., Ohsumi K., Ohnishi I., Nakamura-Messenger
757 K., Nakamura T., Mostefaoui S., Mikouchi T., Meibom A., Matrajt G., Marcus M. A.,
758 Leroux H., Lemelle L., Le L., Lanzirotti A., Langenhorst F., Krot A. N., Keller, L. P.,
759 Kearsley A. T., Joswiak D., Jacob D., Ishii H., Harvey R., Hagiya K., Grossman L.,
760 Grossman J. N., Graham G. A., Gounelle M., Gillet P., Genge M. J., Flynn G., Ferroir T.,
761 Fallon S., Ebel D. S., Dai Z. R., Cordier P., Clark B., Chi M., Butterworth A. L., Brownlee
762 D. E., Bridges J. C., Brennan S., Brearley A., Bradley J. P., Bleuet P., Bland P. A. and
763 Bastien R. (2006) Mineralogy and Petrology of Comet 81P/Wild 2 Nucleus Samples.
764 Science 314, 1735–1739.
765

766

Figure captions

Fig. 1. (A) Optical image of a mechanically isolated olivine grain from Orgueil. (B, C) Defocused optical images of olivine grains showing a potential fluid/melt inclusion near a grain boundary (B) and silicate melt along grain boundaries (C).

Fig. 2. Composite EDX elemental map of Mg (red), Fe (blue), and Ca (green) in a representative section of Ivuna, revealing the preferential distribution of carbonates (green) in the bottom left of the section. Anhydrous silicates were not observed in this section.

Fig. 3. (A) Oxygen three-isotope plot of olivine and carbonate grains from Ivuna and Orgueil CI chondrites. Olivine grains show terrestrial isotopic values except for olivine grain O16-8, which is enriched in ^{16}O and plots on the PCM below the TFL. Carbonate data define a linear trend that is indistinguishable from the TFL within errors [$\delta^{17}O = (0.50 \pm 0.05) \times \delta^{18}O + (0.9 \pm 1.4)$]. Uncertainties shown are 2σ. (B) $\Delta^{17}O$ vs. $\delta^{18}O$ values of components of Ivuna and Orgueil: except for magnetite grains and olivine grain O16-8, all data plot, within errors, on the TFL. Uncertainties shown are 2σ. Data from Clayton and Mayeda, 1984; Rowe et al., 1994; Leshin et al., 1997; Clayton and Mayeda, 1999.

Fig. 4. Distributions of fayalite content (mol. %) for olivine in CI chondrites (data from this study and Reid et al., 1970; Kerridge and MacDougall, 1976; Steele, 1990; Leshin et al., 1997; Le Gac et al., 2009; Frank et al., 2014).

Fig. 5. Probability density functions of the $\Delta^{17}O$ values of silicates in comets and IDPs (n = 146, green) and CI chondrites (olivine and pyroxene, n = 41, orange; see text for references).

Fig. 6. Schematic oxygen three-isotope plot of bulk CM chondrites. The intersection between this trend and the PCM corresponds to the bulk anhydrous O isotope composition of CM

816 chondrites before overprinting by parent-body processes. It should be noted that using the
817 CCAM instead of the PCM does not affect our conclusions within errors.
818
819 **Fig. 7.** (A) Calculated bulk $\Delta^{17}O$ values of primordial carbonaceous chondrites before the
820 onset of aqueous alteration (CM = green, CO = red, CV = blue, and CR = purple). (B)
821 Calculated $\Delta^{17}O$ of primordial, pre-alteration matrices in CM, CO, CV, and CR chondrites.
822 The dashed orange line in both plots corresponds to the CI value ($\Delta^{17}O$ = 0‰). Uncertainties
823 shown in both plots are 2σ. See text for details.

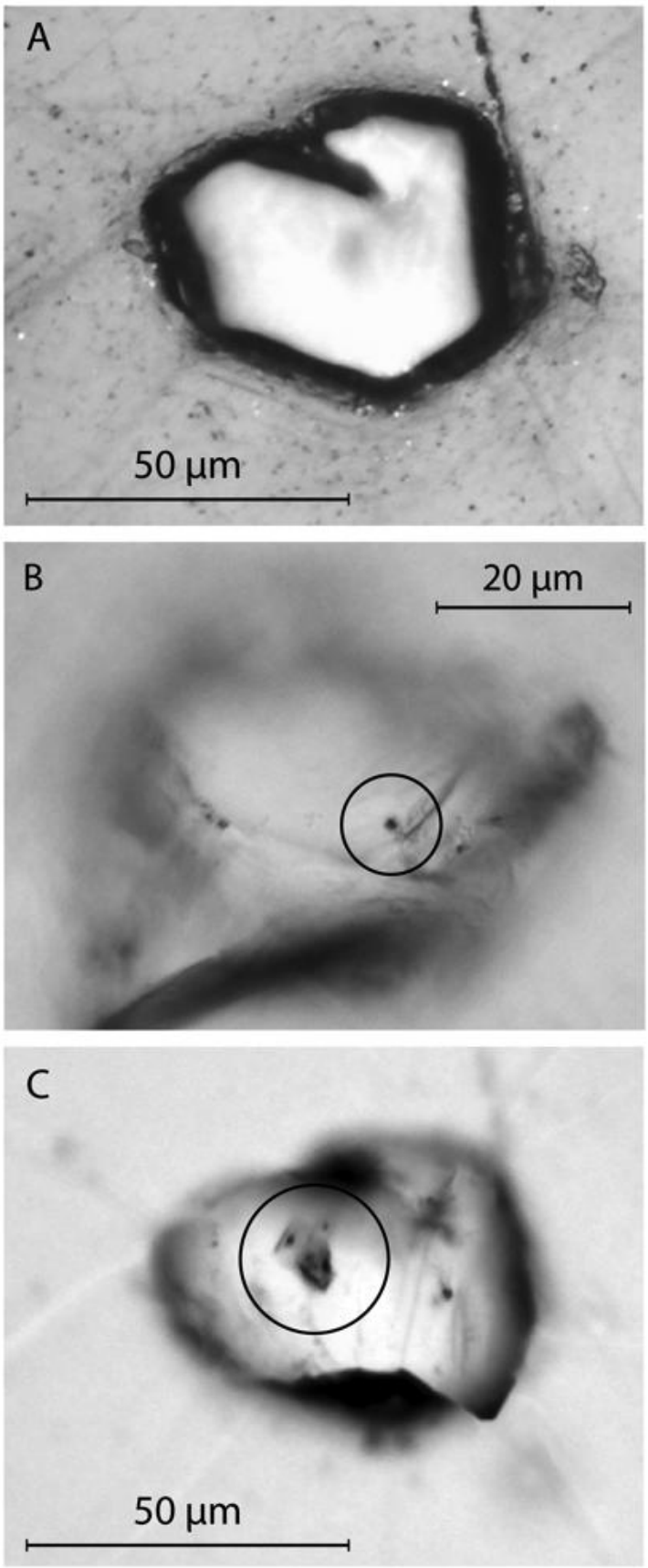

824

825 **Fig. 1**

826

827

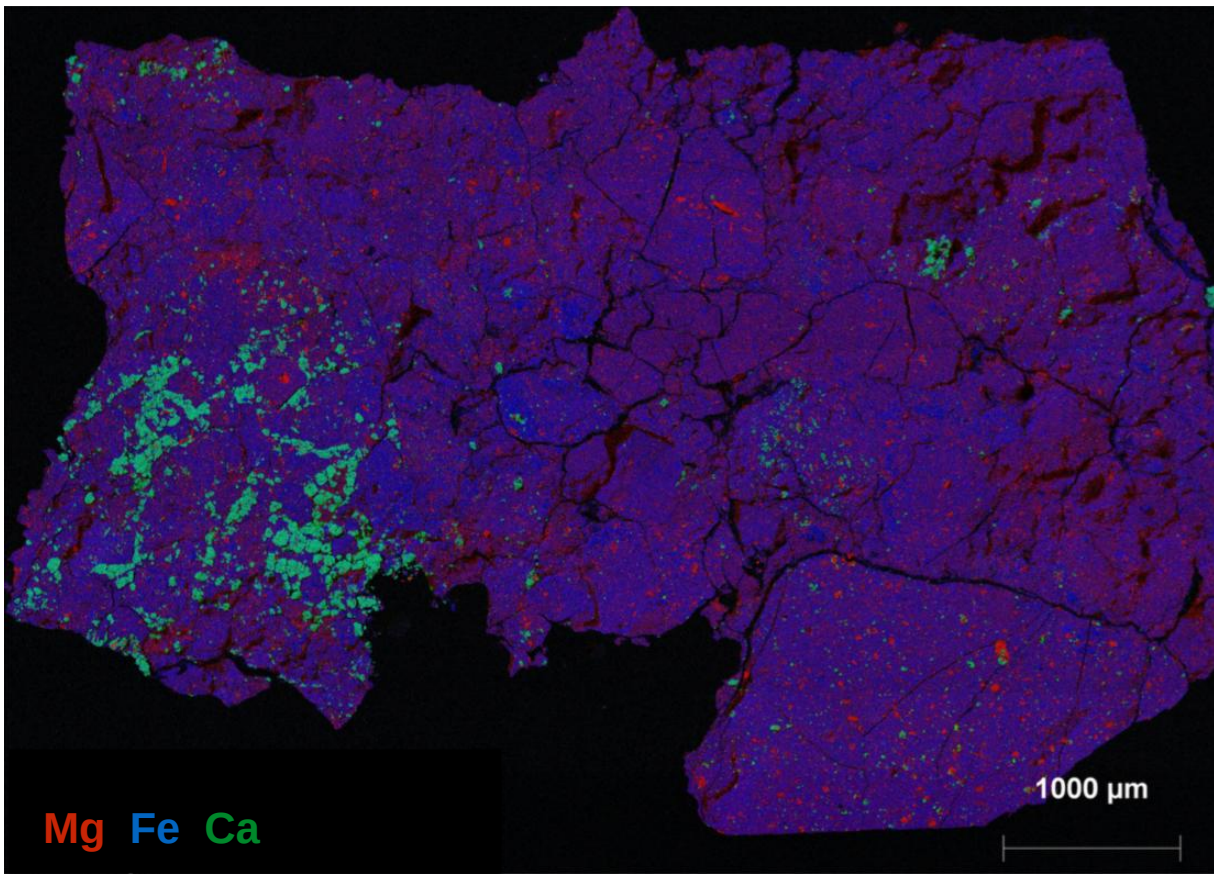

828

829

830 **Fig. 2**

831

832

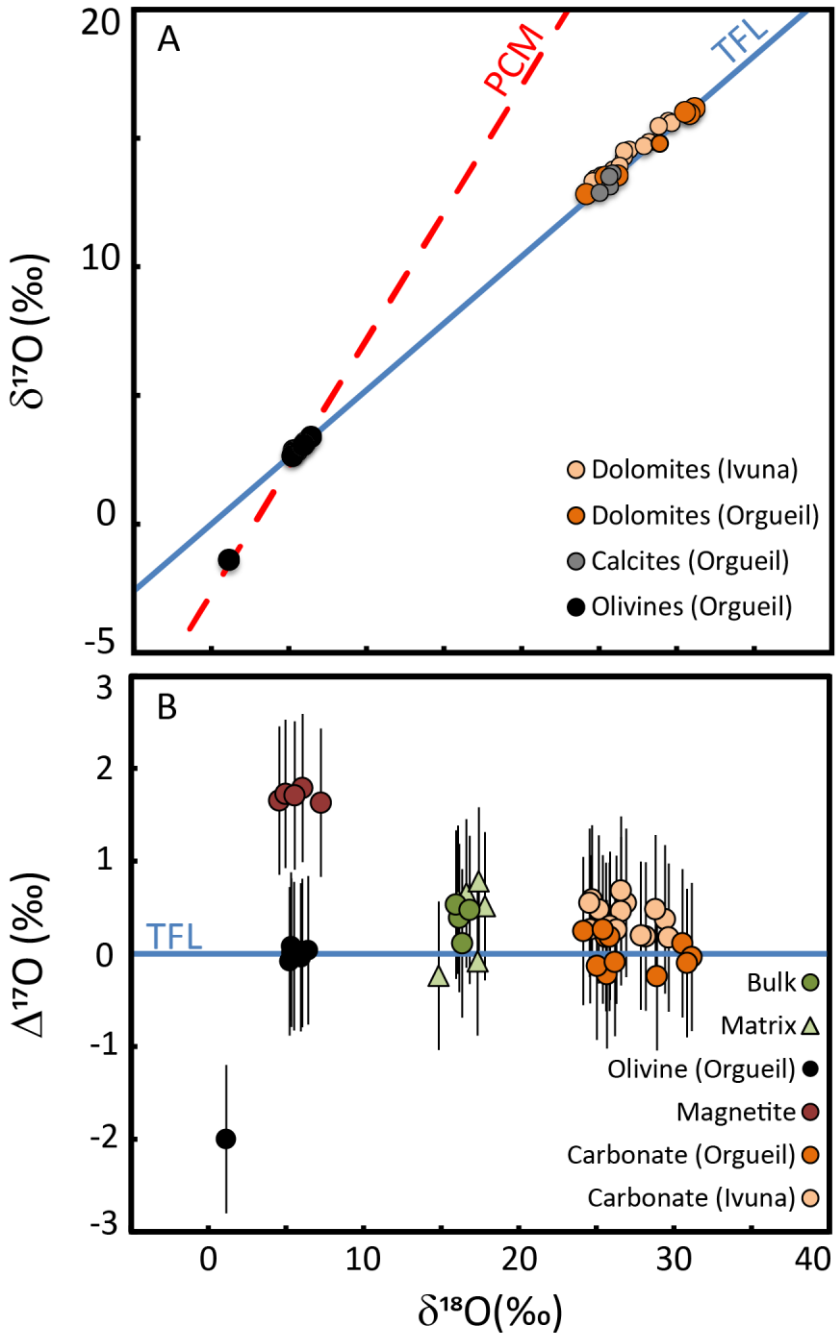

833

834 **Fig. 3**

835

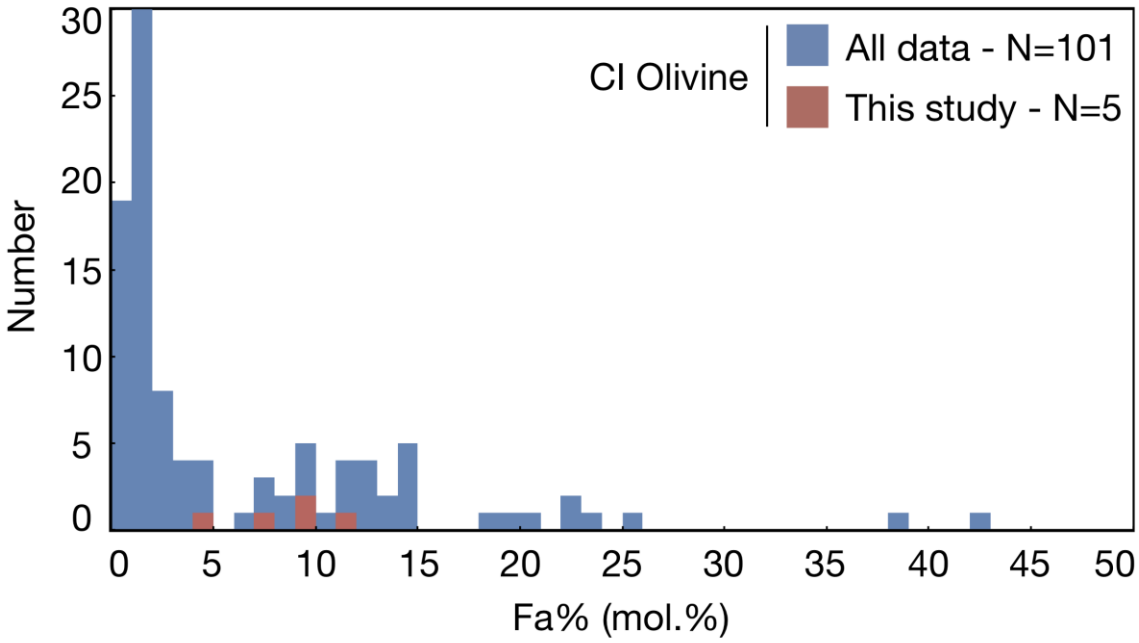

836

837 **Fig. 4**

838

839

840

841

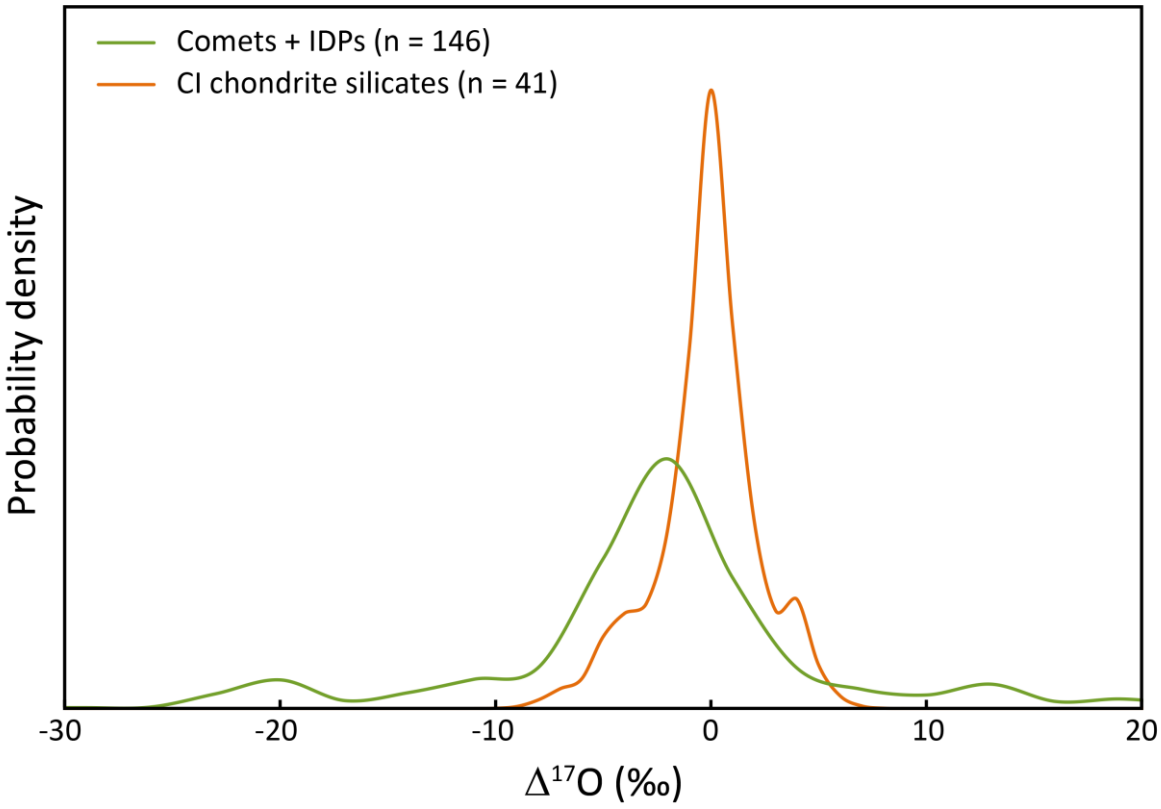

842

843 **Fig. 5**

844

845

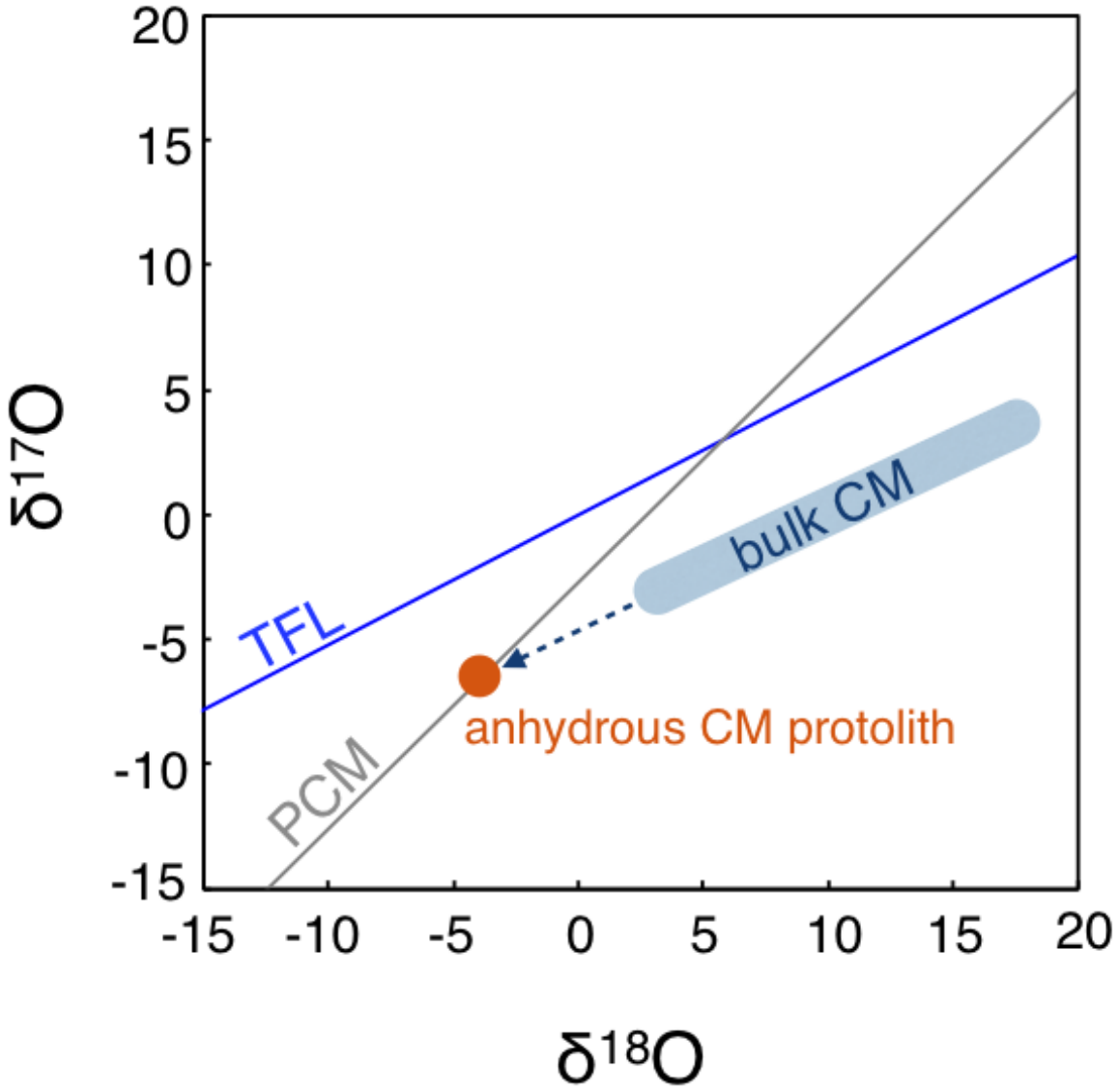

846

847

848 **Fig. 6**

849

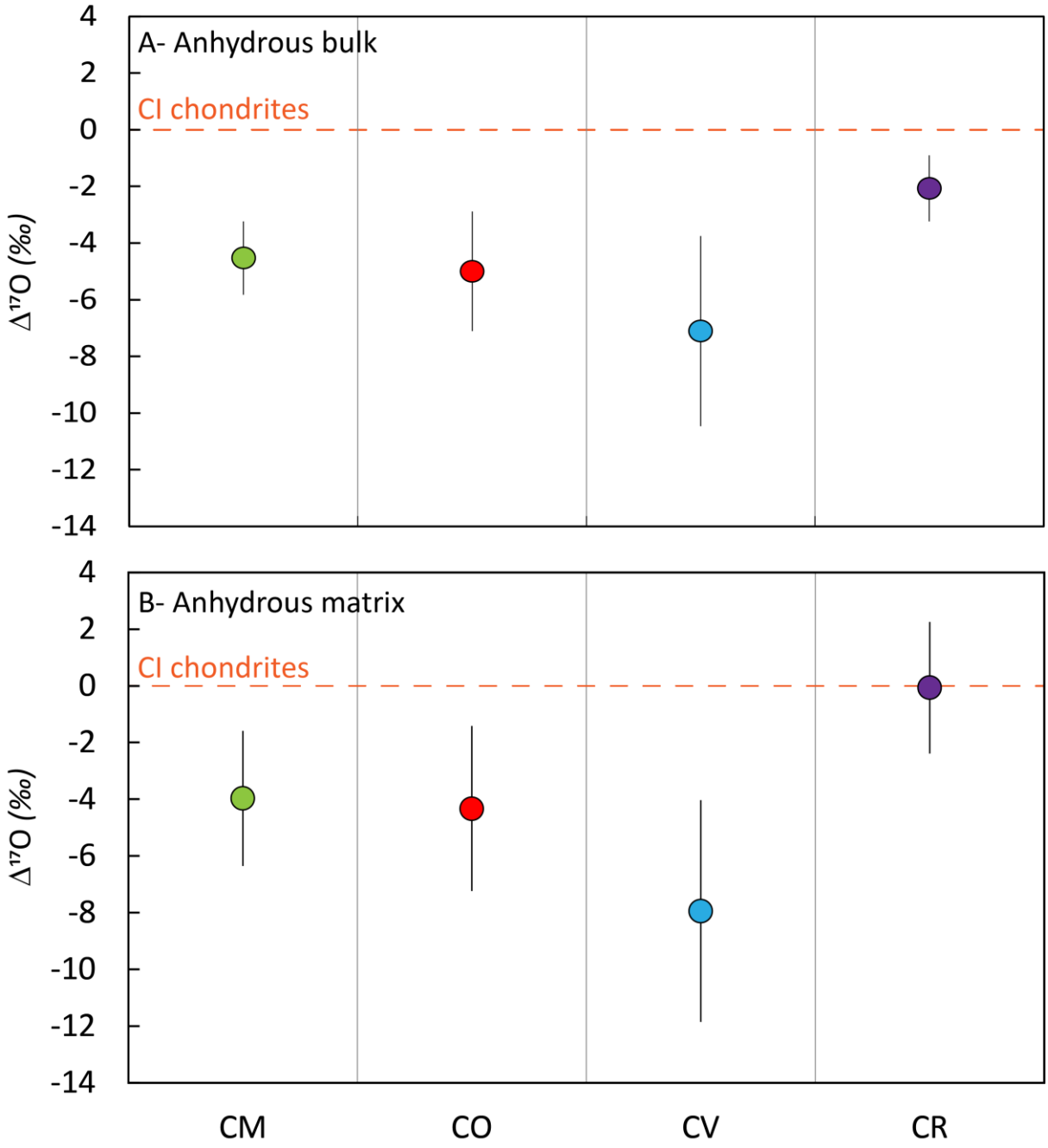
A- Anhydrous bulk
CI chondrites
B- Anhydrous matrix
CI chondrites
Δ17O (‰)
4
2
0
-2
-4
-6
-8
-10
-12
-14
CM
CO
CV
CR

850

851 **Fig. 7**

Meteorite	Mineralogy	Sample	SiO_2	MgO	FeO	Al_2O_3	CaO	Cr_2O_3	MnO	Total	Mg#
Orgueil	Olivine	O6-18	42.9	49.7	9.0	*bdl*	0.1	*bdl*	0.1	101.7	0.91
		O6-23	42.9	49.4	8.9	*bdl*	0.1	*bdl*	0.1	101.5	0.91
		O6-24	42.2	47.4	11.5	*bdl*	0.1	*bdl*	0.2	101.3	0.88
		O16-8	43.8	53.4	4.7	0.2	0.2	0.6	0.1	102.9	0.95
		O21-5	43.8	50.0	7.7	*bdl*	0.1	0.5	0.3	102.4	0.92

Table 1. Chemical compositions and Mg# of olivine mechanically isolated from Orgueil. *Bdl* = below detection limit.

Chondrite	Mineralogy	Sample	wt.%						mol.%						Molar Mg/Ca
			CaO	MgO	FeO	MnO	Na_2O	SiO_2	Ca	Mg	Fe	Mn	Na	Si	
Orgueil	**Calcite**	O21-7	54.56	0.41	*bdl*	*bdl*	*bdl*	*bdl*	98.97	1.03	-	-	-	-	0.0
		O21-8	57.88	0.16	*bdl*	*bdl*	*bdl*	*bdl*	99.63	0.37	-	-	-	-	0.0
		O21-9	56.45	0.27	*bdl*	*bdl*	*bdl*	*bdl*	99.34	0.66	-	-	-	-	0.0
	Dolomite														
		O6-1	27.78	16.37	1.64	3.47	*bdl*	0.11	50.81	41.66	2.33	5.02	-	0.18	0.8
		O6-12	29.05	18.96	1.69	2.10	*bdl*	*bdl*	49.73	45.17	2.25	2.84	-	-	0.9
		O6-17	26.87	18.96	1.75	4.83	*bdl*	*bdl*	46.00	45.14	2.33	6.53	-	-	1.0
		O15-1	27.34	19.27	1.57	3.02	*bdl*	0.37	47.05	46.14	2.11	4.11	-	0.59	1.0
		O15-3	27.76	18.74	1.81	2.66	*bdl*	*bdl*	48.41	45.46	2.46	3.67	-	-	0.9
		O15-5	28.79	19.12	1.50	2.52	*bdl*	*bdl*	49.17	45.43	2.00	3.40	-	-	0.9
		O16-4	27.04	14.78	1.88	5.13	*bdl*	*bdl*	50.91	38.71	2.76	7.63	-	-	0.8
		O16-6	26.79	18.15	1.89	3.71	*bdl*	*bdl*	47.46	44.73	2.61	5.20	-	-	0.9
		O16-7	27.57	19.34	1.76	3.30	*bdl*	0.06	47.13	45.99	2.34	4.45	-	0.09	1.0
		O16-9	25.03	18.69	2.35	5.68	*bdl*	*bdl*	43.64	45.34	3.19	7.83	-	-	1.0
		O17-2	27.51	17.30	1.34	5.18	*bdl*	0.12	48.41	42.35	1.83	7.21	-	0.20	0.9
		O17-7	28.19	17.36	1.80	4.09	*bdl*	0.25	49.27	42.22	2.46	5.65	-	0.41	0.9
		O21-1	30.72	20.00	1.36	3.45	*bdl*	*bdl*	49.28	44.64	1.70	4.37	-	-	0.9
	Ferromagnesite	O6-2	0.18	34.94	11.88	7.01	*bdl*	0.06	0.27	76.37	14.56	8.71	-	0.08	277.8
		O6-7	0.72	28.79	15.14	10.43	*bdl*	0.06	1.18	65.79	19.41	13.54	-	0.08	55.6
		O6-10	0.31	33.94	16.32	3.73	*bdl*	*bdl*	0.48	74.71	20.15	4.66	-	-	154.8
		O7-8	0.19	31.41	16.71	6.32	*bdl*	0.12	0.31	70.44	21.03	8.05	-	0.17	230.0
		O7-13	0.57	31.09	12.49	10.13	*bdl*	0.22	0.91	70.02	15.78	12.96	-	0.32	76.6
		O7-18	0.10	34.38	16.56	2.80	*bdl*	*bdl*	0.15	75.85	20.49	3.51	-	-	503.4
		O17-6	0.30	29.75	21.62	2.72	*bdl*	0.18	0.49	67.98	27.72	3.53	-	0.28	138.0
		O21-6	bdl	47.06	0.51	*bdl*	*bdl*	*bdl*	-	99.40	0.60	-	-	-	-

Ivuna	**Dolomite**	I-1	31.76	19.51	1.47	0.95	*bdl*	*bdl*	52.24	44.64	1.89	1.23	-	-	0.9
		I-2	25.86	18.29	1.93	4.55	0.16	1.05	44.84	44.12	2.61	6.24	0.49	1.70	1.0
		I-3	31.92	19.83	1.28	0.39	0.06	*bdl*	52.40	45.29	1.65	0.50	0.17	-	0.9
		I-4	30.23	20.45	2.17	1.63	0.07	*bdl*	48.92	46.05	2.75	2.09	0.19	-	0.9
		I-5	29.33	19.15	1.25	4.16	*bdl*	*bdl*	48.69	44.23	1.62	5.45	-	-	0.9
		I-6	28.54	20.32	2.06	1.16	0.07	0.11	47.92	47.47	2.70	1.54	0.21	0.17	1.0
		I-7	28.38	20.86	2.19	1.23	0.10	0.40	46.82	47.86	2.81	1.60	0.28	0.62	1.0
		I-8	25.02	21.83	1.49	3.68	0.08	0.26	41.80	50.75	1.95	4.86	0.24	0.41	1.2
		I-9	30.00	18.77	1.98	2.85	*bdl*	*bdl*	50.07	43.59	2.58	3.76	-	-	0.9
		I-10	26.42	17.67	2.69	2.42	0.11	1.05	47.02	43.75	3.74	3.41	0.34	1.75	0.9
		I-11	28.31	19.18	2.09	2.11	*bdl*	0.29	48.33	45.57	2.79	2.85	-	0.46	0.9
		I-12	27.71	18.46	1.51	4.62	*bdl*	0.05	47.55	44.07	2.02	6.27	-	0.09	0.9
		I-13	28.29	19.98	2.11	1.08	0.06	0.16	48.07	47.25	2.80	1.46	0.17	0.26	1.0
		I-14	29.75	20.75	2.20	1.11	*bdl*	0.06	48.56	47.12	2.80	1.43	-	0.09	1.0
		I-15	13.84	23.05	2.56	3.44	0.12	1.28	26.60	61.64	3.83	5.23	0.40	2.29	2.3
		I-16	27.74	18.78	1.54	4.30	*bdl*	*bdl*	47.44	44.69	2.05	5.81	-	-	0.9

Table 2. Chemical compositions of carbonate grains (calcite, dolomite, and ferromagnesite) mechanically isolated from Orgueil. The values of dolomite grains measured in the thick section of Ivuna are also reported (see text for details). *Bdl* = below detection limit.

Meteorite	Mineralogy	Sample	$\delta^{18}O$	2σ	$\delta^{17}O$	2σ	$\Delta^{17}O$	2σ
Orgueil	Olivine	O21-5	6.1	0.2	3.2	0.3	0.0	0.9
			5.5	0.2	2.8	0.3	0.0	0.8
		O6-18	5.3	0.2	2.9	0.3	0.1	0.9
		O6-23	6.4	0.2	3.4	0.3	0.0	0.9
			5.3	0.2	2.8	0.3	0.0	0.8
		O6-24	5.2	0.2	2.6	0.3	–0.1	0.8
			6.0	0.2	3.1	0.3	0.0	0.8
		O16-8	1.1	0.2	–1.4	0.4	–2.0	0.8
	Calcite	O21-7	25.6	0.1	13.5	0.4	0.2	0.8
		O21-8	25.9	0.1	13.6	0.4	0.2	0.9
		O21-9	25.7	0.1	13.1	0.4	–0.2	0.8
		O21-10	25.0	0.1	12.9	0.4	–0.1	0.9
	Dolomite	O21-1	30.6	0.0	16.0	0.2	0.1	0.8
		O17-7	24.2	0.0	12.8	0.2	0.2	0.9
		O16-6	26.2	0.0	13.5	0.2	–0.1	0.9
		O16-9	25.4	0.0	13.5	0.2	0.3	0.8
		O16-7	31.2	0.0	16.2	0.2	0.0	0.8
		O6-12	28.9	0.0	14.8	0.2	–0.2	0.8
		O6-17	30.9	0.0	15.9	0.2	–0.1	0.8
Ivuna	Dolomite	I-1	26.9	0.1	14.5	0.1	0.5	0.8
		I-2	29.4	0.1	15.7	0.1	0.4	0.7
		I-3	26.6	0.1	14.3	0.1	0.5	0.8
		I-4	29.7	0.1	15.6	0.1	0.2	0.7
		I-5	26.6	0.1	14.5	0.1	0.7	0.7
		I-6	28.8	0.1	15.5	0.1	0.5	0.7

I-7	24.7	0.1	13.4	0.1	0.6	0.6
I-8	28.2	0.1	14.8	0.1	0.2	0.6
I-9	25.2	0.1	13.6	0.1	0.5	0.8
I-10	24.6	0.1	13.1	0.1	0.3	0.6
I-11	25.9	0.1	13.8	0.1	0.3	0.6
I-12	27.9	0.1	14.7	0.1	0.2	0.7
I-13	24.6	0.1	13.3	0.1	0.5	0.7
I-14	26.3	0.1	13.9	0.1	0.3	0.8

Table 3. Oxygen isotopic compositions of olivine, calcites, and dolomites mechanically isolated from Orgueil. The oxygen isotopic compositions of dolomite grains measured in the thick section of Ivuna are also reported (see text for details).

		$\delta^{18}O$	2σ	$\delta^{17}O$	2σ	$\Delta^{17}O$	2σ
bulk	CM	–3.9	0.5	–6.6	0.4	–4.5	0.6
	CO	–4.9	0.9	–7.6	0.6	–5.0	1.1
	CV	–9.4	1.3	–12.0	1.1	–7.1	1.7
	CR	1.3	0.5	–1.4	0.3	–2.1	0.6
matrix	CM	–3.0	0.9	–5.5	0.8	–4.0	1.2
	CO	–4.0	1.1	–6.4	0.9	–4.3	1.5
	CV	–11.9	1.5	–14.1	1.3	–7.9	2.0
	CR	4.7	0.9	2.4	0.8	–0.1	1.2

Table 4. Calculated primordial (pre-alteration) bulk and matrix oxygen isotopic compositions for different carbonaceous chondrites. Primordial compositions were calculated from the bulk O isotopic trends (Marrocchi et al., 2018b), the modal abundances of CAIs, chondrules, and matrix (Scott and Krot, 2014), and the average O isotopic compositions of CAIs and chondrules for each type of carbonaceous chondrite (Tenner et al., 2018).